INITIAL INVESTIGATION OF SILICA AEROGEL EQUIPPED ON SM/MPAC & SEED RECOVERED FROM THE ISS IN 2002, 2004, AND 2005

Takaaki NOGUCHI[1], Tomoki NAKAMURA[2], Yukihito KITAZAWA[3,*], Riyo YAMANAKA[4], Yugo KIMOTO[4], and Mineo SUZUKI[4]

[1]*College of Science, Ibaraki University, Mito, Ibaraki 310-8512, Japan*
[2]*Department of Earth and Planetary Science, Faculty of Science, Kyushu University, Hakozaki, Fukuoka 812-8582, Japan*
[3]*IHI Corporation, Toyosu IHI Building, Toyosu, Koto, Tokyo 135-8710, Japan*
[4]*Institute of Aerospace Technology, Japan Aerospace Exploration Agency, Tsukuba, Ibaraki 305-8505, Japan*
**Guest researcher of JAXA/IAT and NiCT, Visiting researcher of JAXA/IASA*

Silica aerogel was equipped on the SM/MPAC (Service Module/Micro-Particle Capturer) to collect both artificial and natural fine-grained particles on the orbit of International Space Station (ISS). We performed initial investigation of the silica aerogel tiles retrieved in 2002, 2004, and 2005. Scanning electron microscope (SEM) observation of the surfaces of the RAM facing tiles revealed that those retrieved in 2004 and 2005 are covered by considerable craters. Each bottom of crater has a wrinkled area. Based on the comparison between them and the surface morphology of silica aerogel reacted with a droplet of ethanol, that these craters were probably formed by low speed impact of liquid droplets. On the surfaces of the WAKE facing tiles, number density of craters is lower than that the RAM facing aerogel. However, their depth/crater diameter ratios are larger than those facing to the RAM direction. We investigated three terminal particles found on the ends of tracks in silica aerogel, retrieved in 2002, 2004, and 2005. Combined SEM, transmission electron microscope (TEM), micro Raman spectroscopy, and synchrotron radiation X-ray diffraction analyses revealed that they are space debris, secondary debris, and a micrometeoroid, respectively.

Keywords: MPAC, Silica aerogel, Space debris, Micrometeoroid

1. Introduction

Silica aerogel is an ultra-low density SiO_2 gel (0.01 to 0.03 g/cm^3). Due to its very low density, it is one of the best media to capture fine-grained particles that move in hypervelocities (ca. 1 to 10 km/s) in space. Because the material is almost colorless and transparent, it is easy to identify captured particles. It has been equipped on manmade satellites on low earth orbits (LEO) (e. g. EuReCa [1]; Orbital debris collector (ODC)-MIR [2]) to collect micrometeoroids and space debris, and on the Stardust spacecraft to collect cometary dust that emitted from 81P/Wild 2 comet (e. g. [3]). Hörz et al. [2] have successfully recovered some micrometeoroids from the aerogel mounted on the ODC on the Mir. Zolensky et al. [4] have also recovered cometary dust originated from 81P/Wild2.

SM/MPAC & SEED (Service Module/ Micro-Particles Capturer and Space Environment Exposure Device) equipped on the international space station (ISS) also contained silica aerogel. SM/MPAC & SEED is composed of three sets of units, each of which is formed by the same modules. Silica aerogels are set in the third and forth modules in a unit. In each unit, 24 silica aerogel tiles faced the RAM side and the same number of silica aerogel tiles faced the WAKE side. Each of the tiles has a 37 x 37 mm exposure area. These three units of the SM/MPAC & SEED have been retrieved from the ISS in 2002, 2004, and 2005. Here we report the initial investigation of the silica aerogel tiles equipped on the ISS and three captured particles (terminal particles) in the silica aerogel tiles. This is the second success of detailed analysis of individual terminal particles in silica aerogel from low earth orbit (LEO).

2. Experimental methods

Silica aerogel tiles are in the third and fourth trays of the SM/MPAC & SEED. The three pairs of RAM and WAKE facing silica aerogel tiles were used for detailed inspection of both their surfaces. Two silica aerogels tiles that set in the same positions in each third tray of the SM/MPAC were selected. One faced the RAM side and another faced the WAKE side. Their positions in each tray are shown in Fig. 1. They are set at the cross point between the D column and third raw facing to both RAM and WAKE sides. Each unit has been retrieved in 2002, 2004, and 2005 after 315, 865, and 1403-day exposure to space, respectively [5]. We use the following abbreviations for each silica aerogel tile in this paper. For example, a silica aerogel tile retrieved in 2004, set in third unit of the MPAC, facing to the WAKE direction, and set in the cross point between the D column and third raw is called as SM2_3WD3.

These silica aerogel blocks were transferred to a clean room (class 1000) at Ibaraki University and they were placed on a special sample holder for scanning electron microscopy (SEM). Scanning electron microscope (SEM) with energy dispersive spectrometer (EDS) at Ibaraki University was used for the observation of these silica aerogel tiles. Low vacuum mode (ambient pressure in the sample chamber: 25 Pa) was

used to prevent the use of carbon coating for SEM/EDS analysis. Accelerating voltages used were 10 and 15 kV. In both cases, we could obtain good backscattered electron (BSE) images.

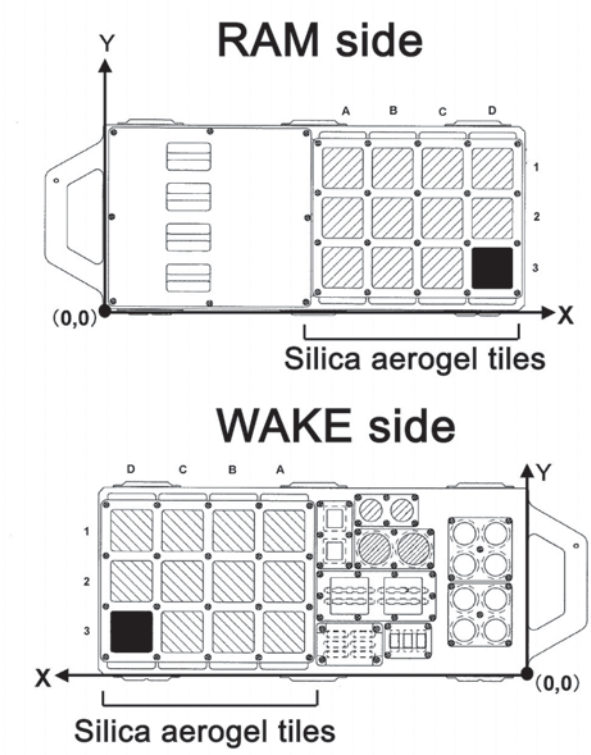

Fig. 1 Positions of silica aerogel tiles used for detailed inspection by using SEM/EDS are indicated by solid symbols. Silica aerogel tiles mounted on third module of each unit of the SM/MPAC & SEED was used for detailed inspection.

During the optical inspection of silica aerogel tiles, it was recognized that several tiles contain remarkable "tracks". "Tracks" are recognized as white straight lines in silica aerogel tiles. Such tracks were formed during hypervelocity capture of fine-grained particles. We selected three tracks containing residual particles at the end of them. Such captured particles are called as "terminal particles" in studies of STARDUST (e. g. [3]). Slabs of silica aerogel that contained tracks were carved out from the tiles. The thickness of the slabs is from 3 to 10 mm thick and depends on the line thickness of the tracks. The slabs were cut out from the tiles at NISSAN ARC LTD. and Ibaraki University. The terminal particles were extracted from the slabs by hand or an electric micromanipulator under a stereomicroscope in a clean bench (class 100) in the clean room.

To characterize the individual terminal particles, synchrotron radiation X-ray diffraction (SR-XRD), micro Raman spectroscopy, transmission electron microscope (TEM), and SEM/EDS were used. Three different methods were applied for each particle. Nondestructive analyses (SR-XRD or micro Raman spectroscopy) were firstly applied and then destructive analysis (TEM and SEM/EDS) were applied. For the terminal particle retrieved in 2004, we utilized SR-XRD at beam line 3A of the Photon Factory Institute of Material Science, High Energy Accelerator Research Organization, Tsukuba, Japan. We could obtain powder diffraction pattern by using Gandolfi camera within 30 minutes. For the other two terminal particles, we utilized to micro Raman spectroscopy to characterize constituent material in the clean room. Excitation wavelength of laser is 785 nm. After these nondestructive analyses, terminal particles were embedded in epoxy resin and ultramicrotomed into 70-nm ultrathin sections by using ultramicrotomes at Ibaraki University. The ultrathin sections were investigated by a transmission electron microscope (TEM) equipped with EDS at Ibaraki University. Accelerating voltage of TEM was 200 kV. The remainders after ultramicrotomy ("potted butts") of the terminal particles were used SEM/EDS to obtain petrographic data from their cross sections.

3. Results

3.1 SEM/EDS analysis of the surface of silica aerogel tiles retrieved in 2002, 2004, and 2005

Silica aerogel tiles facing to the WAKE directions are browner than the RAM facing tiles in all the three units retrieved in 2002, 2004, and 2005. Figure 2 are mosaic photographs of silica aerogel tiles retrieved in 2005 taken under transmitted light. The brown coloring on the WAKE facing tiles retrieved in 2004 and 2005 are quite obvious. The color becomes darker as the exposure time to space increased. Many dark spots can be recognized on the WAKE facing tiles although their real color not always dark. In some cases, their real color is white under reflective light. Coloring shown on the surface of aerogel tiles has been reported in previous studies (e. g. [5], [6], [7]). Both tiles have deep cracks in their central areas. They are probably related to shrinkage of the tiles during return to one atmospheric pressure in the Russian service module because no coloring was observed in the deep interior of the cracks.

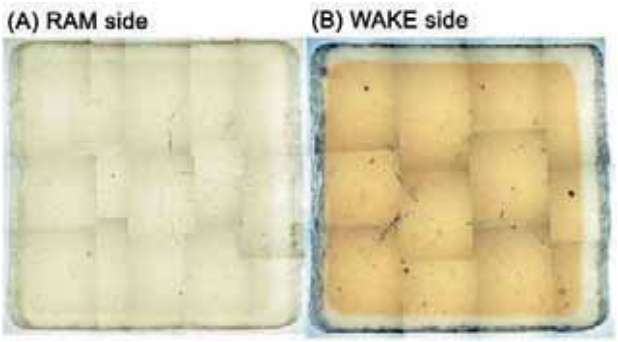

Fig. 2 Mosaic photographs of silica aerogel tiles retrieved in 2005. It is obvious that the WAKE facing tile is browner than the RAM facing one. Many dark spots can be recognized in the WAKE facing tile. The orthogonal lines in both tiles are artifacts due to limb darkening of each photograph.

After optical inspection, the surfaces of the silica aerogel tiles were investigated by SEM/EDS. Figure 3 shows change of surface morphology of the RAM facing silica aerogel tiles and their typical EDS spectra. It is obvious that number density of craters abruptly increased in the second retrieved sample. On the contrary, number densities of craters are not so different between samples retrieved in 2004 and 2005.

Elements except for O and Si derived from silica aerogel were hardly detected. Although a small peak of C Kα was detected from the surface of SM2_3RD3, we could not find C Kα peak from SM3_3RD3 (Figs. 3B, C).

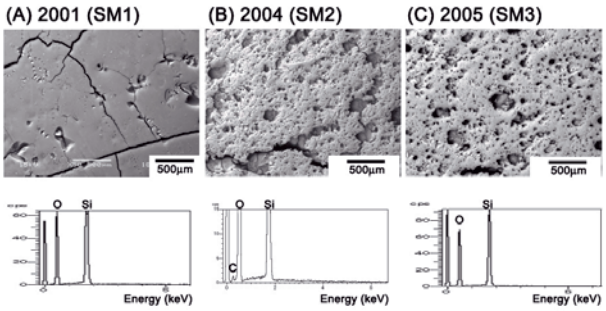

Fig. 3 BSE images of the surface of SM1, 2, and 3_3RD3 tiles and their surface EDS spectra. Detected elements are O and Si derived from silica aerogel itself except for a small peak of C Kα in SM2_3RD3.

Abundant shallow craters observed in SM2 and 3_3WD3 tiles have a common morphological feature. As shown in Fig. 4A, bottom of a crater has a wrinkled area. The wrinkled areas are usually off the center of each bottom. The directions from the center of the bottom to the wrinkled area are similar to each other. Relatively large (typically larger than 200 μm in diameter) wrinkled areas are white under optical microscope when reflective illumination is used (Fig. 4B). We performed several simple experiments to reproduce these features. One of the results is shown in Figs. 4C and D. In this case, a droplet of ethanol was put on the surface of silica aerogel. The droplet was rapidly started to react with silica aerogel. The aerogel tile was promptly placed in a vacuum desiccator and evacuated for 30 minutes. It becomes white under optical microscope and the bottom of the "crater" has wrinkled areas. The morphological similarities between these figures suggest that the abundant shallow craters shown in the RAM facing craters were formed by low speed impacts of liquid droplets.

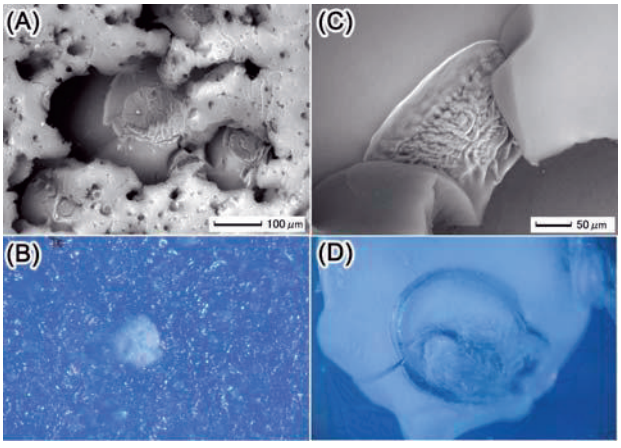

Fig. 4 BSE images and optical photomicrographs of a typical crater on the surface of the RAM facing silica aerogel and reproduction of "a crater" having similar morphology. (A) BSE image of a crater. Bottom of a crater has a wrinkled area and (B) it often corresponds to white stain under optical microscope. Reaction between silica aerogel and a droplet of ethanol formed a dent. (C) The reproduced "crater" (dent) has several wrinkled areas in its bottom and (D) the dent is white under optical microscope.

Figure 5 shows the change in surface morphology of the WAKE facing tiles and their typical EDS spectra. A small amount of C was detected from this side. However, its relative abundances to O or Si were not increased with exposure duration to space. Carbon relative abundance on the tile retrieved in 2005 is the lowest among the tree samples. Therefore it is clear that C content is not directly related to the brown coloring of the WAKE facing tiles. Although elements that constitute the brown color coating were not detected by EDS, the material that probably corresponds to the brown thin coating can be seen in BSE images (Fig. 6). Along the walls of the cracks, we can see at least three "layers" that cover the surface of the tile. Upper "layers" seem to be thicker than the lower "layers".

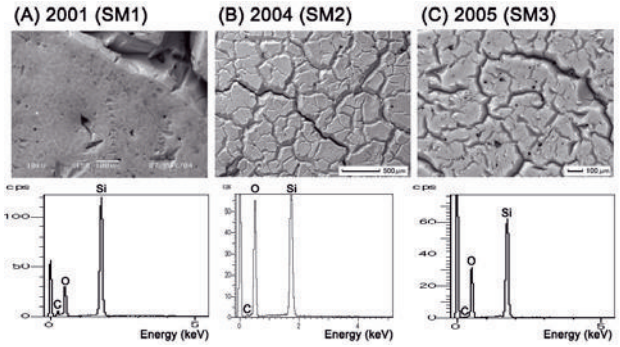

Fig. 5 BSE images of the surface of SM1, 2, and 3_3WD3 tiles and their surface EDS spectra. Detected elements are O and Si derived from silica aerogel itself and a small peak of C.

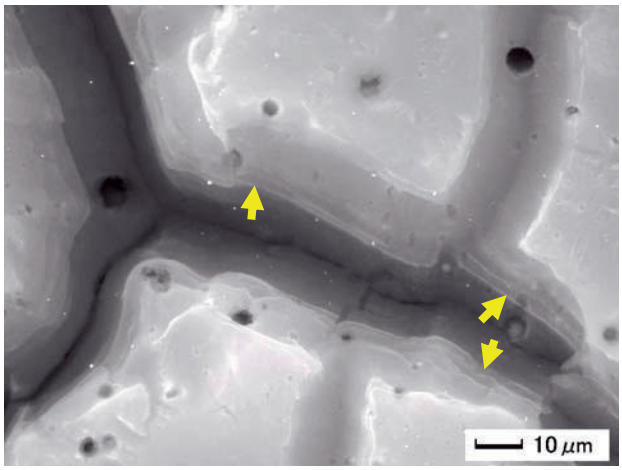

Fig. 6 An enlarged BSE image of cracks in SM3_3WD3. As propagation of cracks into the interior of the silica aerogel tile, the thickness of the coated material seems to be different.

On the WAKE face tiles, we also observed abundant craters as well as cracks. Figures 7A and C are distribution of craters on the RAM and the WAKE facing tiles. Because the number density of craters in the RAM facing tiles is quite high, positions of craters larger than 250 μm in diameter were plotted. On the other hand, craters larger than 100 μm in diameter were plotted in the case of the WAKE side. Even though, the number density of craters in the RAM side is higher than that in

the WAKE side. In addition to the difference in number density of craters, there is an obvious difference in morphology of crates between the RAM facing and the WAKE facing tiles. As can be estimated from Figs. 7B and D, the ratios between depth and diameter of craters are obviously different. The craters on the WAKE side have higher depth/diameter ratios than those on the RAM side. In Fig. 7D, the deep crater also has a wrinkled area in its bottom. The similarity of the morphology of the bottom of craters facing both sides suggests that craters on the WAKE side were also formed by the impacts of liquid droplets. Different depth/diameter ratios between the both sides were probably related to the difference in impact speeds. Formation mechanism of the craters and brown layer will be discussed in chapter 4.

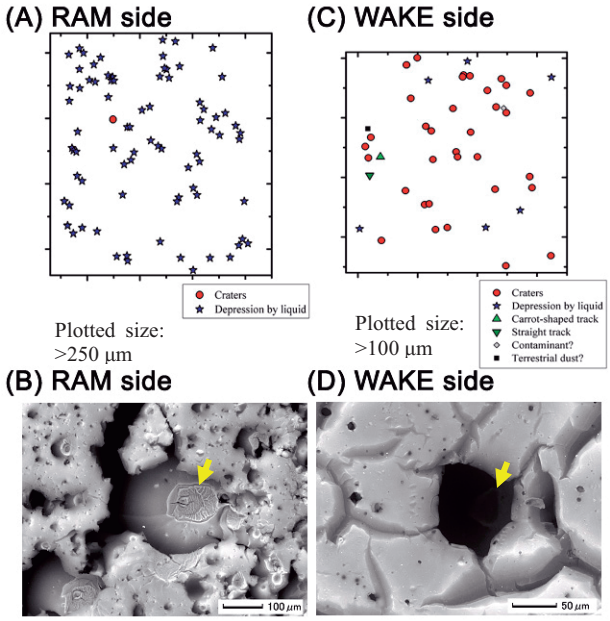

Fig. 7 Distribution of craters on the SM3_3RD3 and SM3_3WD3 tiles and typical morphology of craters in these tiles (BSE images). (A) and (C) Deep craters are plotted by red circles and shallow craters are plotted by blue stars. (B) and (D) Both craters have a wrinkled area in their bottom as indicated by yellow arrows.

3.2 Detailed analyses of terminal particles retrieved in 2002, 2004, and 2005

During optical inspection of silica aerogel tiles at IHI Aerospace LTD, we found many tracks that are easily identified by naked eyes. We identified some tracks that contain particles on their ends. As initial investigation of such captured particles, we selected three aerogel tiles retrieved in 2002, 2004, and 2005. First track is in SM1_3RA1, a tile facing to the RAM side and retrieved in 2002. Second track is in SM2_4WD1, a tile facing to the WAKE side and retrieved in 2004. Third one is in SM3_3WC1, facing to the WAKE and retrieved in 2005. As shown in Fig. 8, the sizes and shapes of the tracks are various. In the first sample, the track is straight and 3.95 mm in length. According to [8], entry speed of the particle that makes this track was estimated to be < 2km/s. The other two are typical "carrot-shaped" tracks. Their lengths are 9.43 and 14.74 mm, respectively. Their entry speeds was estimated to be from 6 to 8 km/s [8]. Recent studies revealed that the effect of frictional heating during capture of fine-grained particles is quite different [9], [10]. The surfaces of the captured particles are heated around 1250 ^{o}C when they are shot at > 6 km/s. On the contrary, particles shot at about 2 km/s, their surfaces are not heated higher than 450 ^{o}C. Therefore, we investigated not only constituent materials of each captured grains but also compared the results with those of the capture experiments. Because all the captured particles investigated in this study exist at the end of the tracks, they are terminal particles. Their sizes are about 5, 50, and 40 μm in length, respectively.

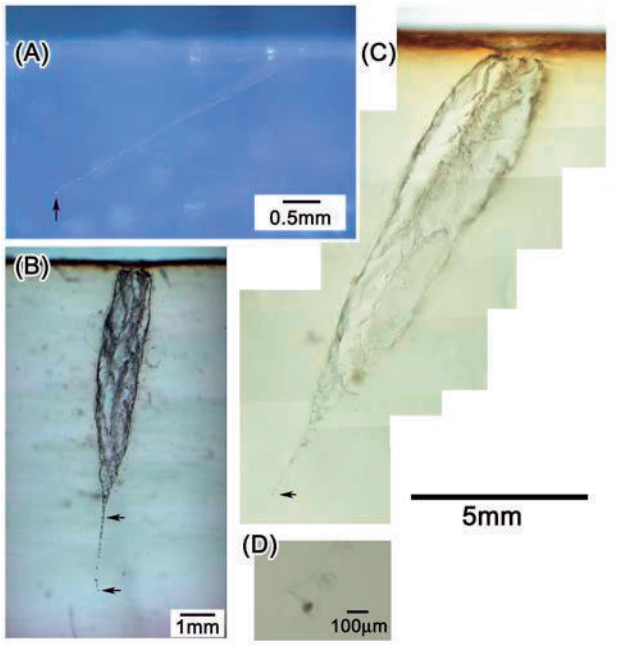

Fig. 8 Photomicrographs of tracks investigated in this study. Terminal particles are indicated by black arrows. (A) SM1_3RA1, (B) SM2_4WD1, (C) SM3_3WD1, (D) an enlarged image of the terminal particle in the track shown in (C).

Raman spectrum of the terminal particle, SM1_3RA1_TP, was obtained. Many Raman shift peaks were obtained from the terminal particle. Major peaks are 531.4, 670.1, 840.7, 980.0, 1092.1, 1284.9, 1593.0 cm^{-1}. Because chemical compositions of the material that emitted these Raman shift peaks are unknown, it is difficult to attribute these peaks to specific vibrations at present. However, based on Raman characteristic group charts, some of these peaks may be related to S and/or N bearing characteristic groups [12]. After ultramicrotomy, a cross section of the terminal particle was investigated by SEM/EDS. EDS analysis of the cross section revealed that it is contains S as well as abundant Al. Therefore, it is estimated that the particle is composed of Al- and S-bearing organic material.

Low magnification bright field image of an ultrathin section of the terminal particle is shown in Fig. 9A. It is composed of polycrystalline metallic Al and Al- and S-bearing amorphous material. Grain size of each Al crystal is < 200 nm across. The amorphous material has a vesiculated texture

throughout the particle. Because no vesiculation occurred during TEM observation, the vesiculation occurred before or during capture by aerogel. Very thin (< 50 nm thick) and non-vesiculated layer of silica aerogel is attached to the surface of the particle. It is similar to attached silica aerogel when projectiles were shot < 2 km/s.

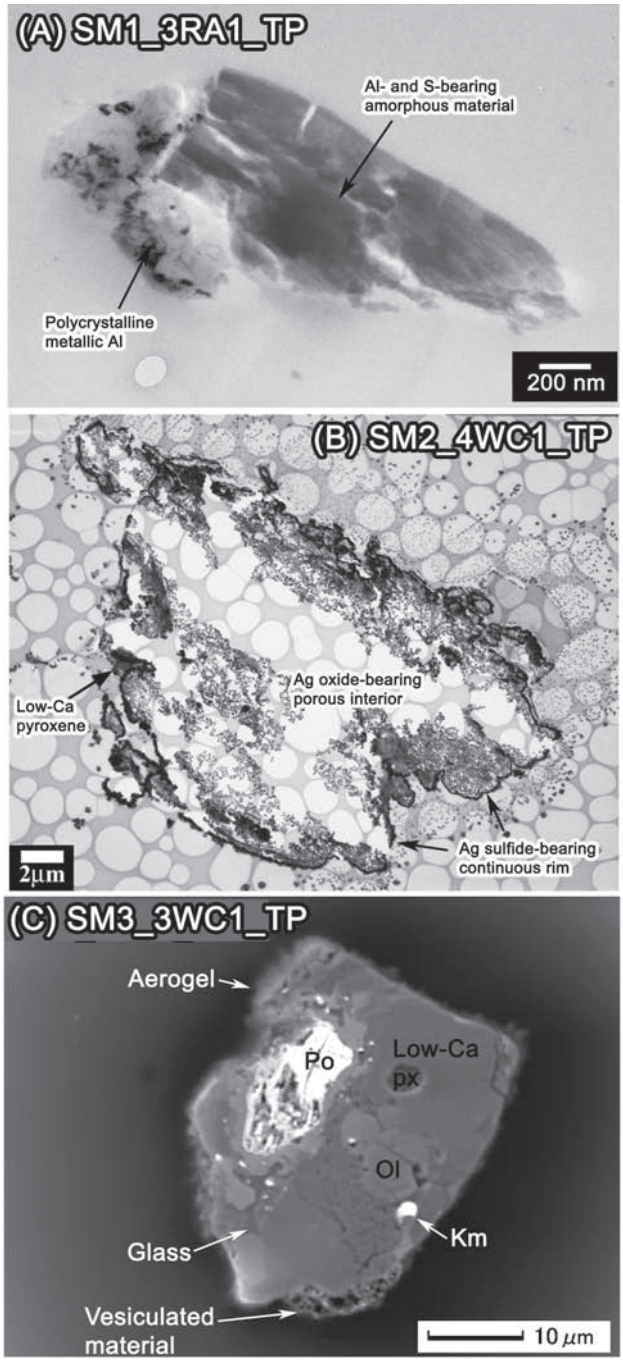

Fig. 9 Cross sections of the terminal particles investigated in this study. (A) and (B) low magnification bright field images of SM1_3RA1_TP and SM2_4WD1_TP. (C) BSE image of SM3_3WC1_TP. Network in (B) is a plastic film containing many holes, which support ultrathin sections. Many aligned sub-μm-sized particles shown in the upper right side of the ultrathin section are Ag oxide, which were fallen out of the loose interior of the terminal particle.

There are two terminal particles in the silica aerogel retrieved in 2004. As indicated by two arrows in Fig. 8B, they were trapped in the funnel-shaped narrow part of the track. A black and opaque grain was trapped in the middle of the narrow channel and another colorless and transparent one was set near the end of the channel. After extraction from silica aerogel, they were investigated by SR-XRD. The black particle was a mixture of silver oxide and sulfide. However, the other one is amorphous. SEM/EDS analysis of these grains after SR-XRD indicates that the latter is basically composed of Si and O. Therefore, in the following section, only the black grain is described. TEM observation of the grain revealed that it has a continuous rim (< 500 nm thick) and a quite porous interior. The rim is composed of S-rich amorphous material and silver sulfide Ag_2S. Its crystal structure is the same as acanthite. Because it is stable below 179 °C, it was transformed from a high temperature form. Amorphous S-rich material among Ag_2S was quite unstable and decomposed under electron beam.

It is quite interesting that the terminal particle contains a 2-μm-wide low-Ca pyroxene crystal near an edge of the particle (Fig. 9B). Because this particle is comprised of a mixture of natural and artificial materials, this particle is secondary debris, which was formed by a collision of a micrometeoroid with an artificial object. Selected area electron diffraction (SAED) pattern and high magnification images of the low-Ca pyroxene crystal show that it is orthopyroxene with many stacking disorders normal to a* direction. Chemical composition of the pyroxene crystal is plotted in Fig. 10. Its composition is $Wo_1En_{84.7}Fs_{14.3}$. Its origin will be discussed in chapter 4.

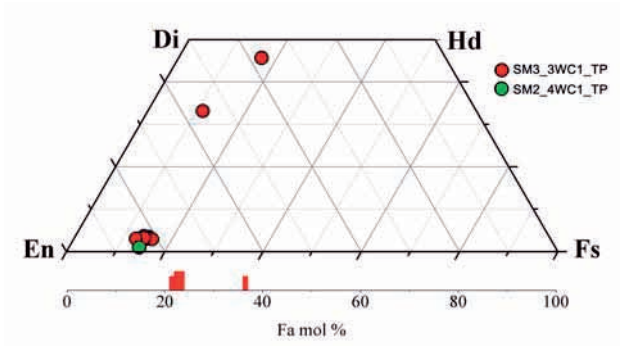

Fig. 10 Chemical compositions of pyroxene and olivine in SM3_4WC1_TP and a pyroxene crystal in SM2_4WD1_TP.

Third terminal particle retrieved in 2005 was set in the end of one of the largest tracks found among silica aerogel tiles retrieved in this year. It was back and opaque and has vitreous luster, suggesting abundant glass on its surface. Micro Raman spectrum of the particle has weak peaks of olivine, low-Ca pyroxene, and amorphous carbon as well as large background probably due to abundant glass on its surface. Presence of olivine and pyroxene suggests that this is a micrometeoroid (natural extraterrestrial particle). Figure 9C is a BSE image of the cross section of the particle. By considering EDS spectra of the particle, the most abundant mineral is low-Ca pyroxene. Most of the olivine crystals are poikilitically enclosed in low-Ca pyroxene. There is glass among these low-Ca pyroxene and olivine crystals. The texture of low-Ca

pyroxene, olivine, and glass strongly suggests that the glass was not formed during frictional heating during capture in silica aerogel. Fe-bearing sulfide and Fe-Ni metal (probably kamacite) are also observed. Aerogel is observed as ~2-μm-thick layer on the surface of the particle. In the lower middle of Fig. 9C, vesiculated material is attached on the surface of the particle. It was probably formed by melting and vesiculation of fine-grained material that enclosed this coarse-grained (> 30 μm across) terminal particle before colliding a silica aerogel tile.

SEAD patterns of constituent minerals in this particles revealed that it is composed of orthopyroxene, olivine, Ca-rich plagioclase, Ni-bearing pyrrhotite, troilite, and taenite. Orthopyroxene and high-Ca pyroxene have homogeneous chemical compositions. The average composition of orthopyroxene is $Wo_{3.1}En_{82.7}Fs_{14.2}$. Average Al_2O_3, Cr_2O_3, and MnO contents of orthopyroxene are 2.6, 1.4, and 0.6 wt %, respectively. Diopsidic high-Ca pyroxene contains 1.7 wt % TiO_2, 2.2 wt % Al_2O_3, 1.9 wt % Cr_2O_3, and 0.7 wt % MnO. Most olivine crystals are also equilibrated except for one crystal. Their average Fa mol % is 25.1 and their average MnO is 0.9 wt %. Unfortunately, stoichiometry of plagioclase is bad probably due to partial decomposition by frictional heating during capture in silica aerogel. Ni-bearing pyrrhotite exists with troilite. Its composition is $Fe_{32.7}Ni_{12.1}S_{55.2}$. SAED pattern of the crystal shows a=2A and c=3C super lattice diffraction. Such super lattice diffractions are often observed among Fe-rich sulfides in interplanetary dust particles, typically ~15-μm-sized extraterrestrial material captured in the stratosphere [12].

4. Discussion

4.1 Contamination on the silica aerogel tiles

Brown coloring has been also reported in the SM/MPAC & SEED experiments (e. g. [5], [6], [7]). They found that (1) contamination is more severe on the RAM side than on the WAKE side, (2) major contamination on the RAM side is continuous SiO_x layer, whose thickness increased with the increase of exposure duration, (3) that on the WAKE side are brown coating and many spotty stains. The SiO_x layer was estimated to have been produced by atomic oxygen (AO) reaction with siloxane. Based on the morphology, numerous colored spots were expected to have been formed by the particles and/or liquid droplets. Because two brown spots contained abundant N or F, fuel/oxidizer reaction products (FORP) were thought to be causes of these spots.

Our observation and a simple simulation experiment suggest that craters with wrinkled bottoms were formed by low-speed impact of liquid droplets. It is consistent with the above investigations. However, our observation revealed number density of such craters is much higher on the RAM facing tiles than on the WAKE facing ones. Because abundant "spots" were not detected on the RAM facing surface of aluminum plates by optical inspection and XPS analysis, chemical compositions of liquid droplets impinged between on the RAM side and on the WAKE side would have been different. Because the silica aerogel tiles are hydrophobic, the aqueous solution droplets would not have formed the craters.

We also found that the impact speeds of liquid droplets on the WAKE side were probably higher than those on the RAM side. This estimation is consistent with the previous works because the WAKE facing MPAC & SEED must have severely experienced thruster plumes of Progress braking thrusters [5]. This means that the WAKE facing silica aerogel tiles suffered impacts by higher speed droplets and/or particles from the plumes. However, it is still an enigma that why the RAM facing tiles experienced more abundant impacts of liquid droplets than the WAKE facing tiles although the speeds of droplets were lower than the latter. One important fact that may serve to estimate the origin of "projectiles" of the crates on the RAM side is that most of the wrinkled area in each crater offsets in the same direction (Fig. 4A). It means that the liquid droplets always came from almost the same direction or formed by single event. We need to search the sources of the projectiles of the craters on the RAM side, other than FORP.

SEM observation of the surface of the WAKE facing tiles revealed that contamination layer that probably corresponds to the brown coating under optical microscope proceeded several times based on the texture of cracks coated by contamination (Fig. 6). If the coated material and "projectiles" of the craters had been formed by the same material, thickness of the coated material and the number density of the craters would have increased in a discontinuous manner. If the origin of this material had been thrust plumes, liquid droplets directly reached the surface of the tiles would have made deep craters and gaseous material reached the surface of the tiles at a low speed would have made a continuous layer.

4.2 Origin of the space debris and the secondary debris

The main purpose of MPAC is capture of space debris and micrometeoroids on the ISS. In spite of the severe contamination on silica aerogel tiles as described above, there are tracks that capture fine-grained particles on their ends. Our investigation of the terminal particles confirmed that both space debris and micrometeoroids can be captured and that we can obtain important information from the particles. First terminal particle retrieved in 2002 is a mixture of metallic aluminum and Al- and S-rich amorphous material. Second one is a mixture of silver oxide and sulfide as well as a small fragment of orthopyroxene (natural crystal). Their origins are hard to estimate because there is no database of materials that can be obtained as fine-grained space debris. An idea of the origin of the first particle is partially reacted solid propellant because metallic Al is used as a metallic fuel. The origin of second particle is even hard to be deduced. One possible idea of its origin might be an electrode of a solar panel.

4.3 Origins of orthopyroxene in the secondary debris and the micrometeoroid

We could obtain a micrometeoroid from an aerogel tile retrieved in 2005. There are only a few micrometeoroids investigated by TEM [2]. All micrometeoroids investigated in [2] were aggregates composed of more than two kinds of minerals. They contained olivine exhibiting sharp electron-diffraction spots indicative of well crystalline and of minimal shock-deformation. One terminal particle contained

olivine, high-Ca pyroxene (augite and diopside), troilite, spinel-group minerals (chromite, magnetite, and hercynite). Olivine was contained in two terminal particles and compositional ranges of olivine were $Fo_{60–70}$ and $Fo_{39–53}$, respectively. On the other hand, the micrometeoroid found in this study has a texture similar to porphyritic olivine pyroxene chondrules, some coarse-grained Antarctic micrometeorites (AMMs) [13], and some coarse-grained terminal grains retrieved from Wild2 comet by STARDUST spacecraft [14]. In other words, the micrometeoroid was once melted in space. This is the first successful comparison of the texture of a micrometeoroid and the other extraterrestrial material. The particle contains abundant orthopyroxene, suggestive of equilibrated ordinary chondrites in origin. However, average ferrosilite mol % of the orthopyroxene is 14.2 and below the range of H chondrites ($Fs_{15-17.5}$). Minor elements concentrations (Al_20_3, Cr_2O_3, and MnO) of the orthopyroxene and high-Ca pyroxene are considerably higher than those in H chondrites. Average chemical composition of olivine ($Fa_{25.1}$) coexisting orthopyroxene is also different from that of equilibrated H chondrites (Fa_{16-20}). If orthopyroxene and olivine in the particle was equilibrated, olivine should be more magnesian. Therefore, it is clear that this particle did not experience thermal metamorphism that resulted in equilibrated Fe-Mg partition between them.

The micrometeoroid contains Ca-rich plagioclase and Ni-bearing pyrrhotite, both of which are absent among equilibrated ordinary chondrites. These lines of evidences definitely indicate that this micrometeoroid has no genetic relationship with equilibrated ordinary chondrites. Ni-bearing pyrrhotite is common among carbonaceous chondrites and hydrated interplanetary dust particles, and phyllosilicate-rich AMMs that experienced heavy aqueous alteration on their parent bodies [15]. In this micrometeoroid, primary glass and Ca-rich plagioclase do not show the evidence of aqueous alteration although glass and plagioclase are susceptible to suffer aqueous alteration. Therefore, presence of Ni-bearing pyrrhotite suggests the possibility of aqueous alteration to a minor degree.

On the other hand, orthopyroxene found in the secondary debris has overlap chemical composition of orthopyroxene in ordinary chondrites. Therefore, there is a possibility that the micrometeoroid that made the secondary debris was derived from H chondrite parent body.

These particles collided to the WAKE facing tiles. The shapes of tracks that these two particles were trapped are carrot-shaped and the relative speed to the tiles was from 6 to 8 km/s based on ground-based experiments [8]. Because orbital speed of the ISS is 7.7 km/s, the speeds of the particles at the orbit of the ISS were probably 13.7 to 15.7 km/s. Interplanetary dust particles having atmospheric entry velocities from 14 to 18 km/s are difficult to estimate their parent bodies (asteroidal or cometary) [16]. Therefore, further investigations of the micrometeoroid such as TEM investigation of fine-grained matrix and oxygen isotopic analysis by SIMS are needed to confine its origin.

5. Comments for future MPAC experiment

As shown in the previous section, we often felt difficulty to estimate the origins of fine-grained space debris. Before start of future MPAC experiment such as JEM/MPAC & SEED, it is desired to make a database of materials that can be obtained as fine-grained space debris. At the same time, further investigation of surface contamination by XPS, TOF-SIMS, and so on are also desired. Another important thing to improve is to develop the method to cutout silica aerogel slabs from tile in order to decrease large-sized destruction of tiles during cutout.

6. Conclusions

We investigated silica aerogel tiles faced both the RAM and WAKE sides retrieved in 2002, 2004, and 2005. Although all the tiles suffered contamination, tiles retrieved in 2004 and 2005 were severely contaminated. On the surface of the RAM facing tiles, they experienced heavy bombardment of low speed impacts of liquid droplets. Thick SiO_x layer reported from the other researchers (e. g. [6], [7], [8]) could not be identified because silica aerogel is composed mainly of SiO_2. On the surface of the WAKE facing tiles, brown colored thin film coated the surface. In spite of its identification by both optical microscope and BSE images, we could not identify specific elements derived from the coating. As well as the thin coating, the surface also experienced bombardment of liquid droplets. Even the deep craters on the WAKE side tiles were not formed by hypervelocity impacts because none of them are not carrot-shape or bulbous-shape, indicative of hypervelocity. The depth/crater diameter ratios increase as the speeds of projectiles increase in such velocity range. Because the craters on the WAKE side have larger depth/crater ratios, the craters were probably formed by higher speed liquid impingent than on the RAM side. It is consistent with the severe effect of thruster plume from Progress on the WAKE side.

We could investigate three terminal particles that trapped on the end of tracks in the tiles retrieved in 2002, 2004, and 2005 irrespective of severe contamination. They are space debris, secondary debris, and micrometeoroid based on TEM and the other microanalyses. An orthopyroxene grain found in the artificial material (a mixture of silver oxide and sulfide) testifies that it is a secondary debris. This is the first identification of secondary debris by using microanalysis.

Mineralogy and petrography of the micrometeoroid were investigated in detail. Its texture is similar to chondrules, crystalline AMMs, and coarse-grained terminal particles retrieved by STARDUST. Its constituent minerals are similar to carbonaceous chondrites experienced minor aqueous alteration although no hydrated minerals were identified. However, at present, it is difficult to state whether this micrometeoroid is asteroidal or cometary in origin. Further investigation is needed to restrict the possible origin.

References

[1] M. J. Burchell, R. Thomson, and H. Yano: Capture of hypervelocity particles in aerogel: in ground laboratory and

low Earth orbit, *Planet. Space Sci. 47*, 189-204 (1999).

[2] F. Hörz, M. E. Zolensky, R. P. Bernhard, T. H. See, and J. L. Warren: Impact Features and Projectile Residues in Aerogel Exposed on Mir, *Icarus 147*, 559-579 (2000).

[3] D. E. Brownlee and 182 coauthors: Comet 81P/Wild 2 Under a Microscope, *Science 314*, 1711-1716 (2006).

[4] M. E. Zolensky and 74 coauthors: Mineralogy and Petrology of Comet 81P/Wild 2 Nucleus Samples, *Science 314*, 1735-1739 (2006)

[5] C. Pankop, K. Smith, C. Soares, R. Mikatarian, and N. Baba: Induced contamination onto JAXA's micro-particle capturer and space environment exposure device – Comparison of predictions and measurements, *Proc. 10th ISMSE*, ESA-SP-616 (2006).

[6] N. Baba, M. Suzuki, I. Yamagata, Y. Kimoto, and J. Ishizawa: Experimental Contamination Observation on the Micro-particles Capturer and Space Environmental Exposure Device, *Proc. 10th ISMSE*, ESA-SP-616 (2006).

[7] J. Ishizawa, K. Mori, F. Imai, I. Yamagata and M. Suzuki: Results of the space-environment exposure experiment "SM/MPAC&SEED" on the international space station (2): Siloxane coated polyimide films, and silicone based paints and adhesives, *Proc. 10th ISMSE*, ESA-SP-616 (2006).

[8] Y. Kitazawa, A. Fujiwara, T. Kadono, K. Imagawa, Y. Okada, and K. Uematsu: Hypervelocity impact experiments on aerogel dust collector, J. Geophy. Res. 104, E22035-22052 (1999).

[9] K. Okudaira, T. Noguchi, T. Nakamura, S. Sugita, and H. Yano: Evaluation of mineralogical alteration of micrometeoroid analog materials captured in aerogel. *Adv. Space Res. 34*, 2299-2304 (2004).

[10] T. Noguchi, T. Nakamura, K K. Okudaira, H. Yano, S. Sugita, M. J. Burchell: Thermal alteration of hydrated minerals during hypervelocity capture to silica aerogel at the flyby speed of Stardust. *Meteoritics Planet. Sci. 42,* 357-372 (2007).

[11] G. Socrates; Infrared and Raman characteristic group frequencies, John Wiley and Sons, Ltd, New York, 347 pp. (2001).

[12] J. P. Bradley: Interplanetary dust particles, In: *Meteorites, Comets, and Planets* (A. M. Davis, ed.), Elsevier-Pergamon, Oxford, 689-711 (2005).

[13] G. Kurat, C. Koebel, T. Presper, F. Brandstätter, and M. Maurette: Petrology and geochemistry of Antarctic micrometeorites, *Geochim. Cosmochim. Acta 58*, 3879-3904 (1994).

[14] T. Nakamura and 11 coauthors: Mineralogy, Three Dimensional Structure, and Oxygen Isotope Ratios of Four Crystalline Particles from Comet 81P/Wild 2 *Lunar Planet. Sci. XXXIX*, Abstract #1695 [CD-ROM] (2008).

[15] M. E. Zolensky and K. Thomas: Iron and iron-nickel sulfides in chondritic interplanetary dust particles. *Geochim. Cosmochim. Acta* 59, 4707-4712 (1995).

[16] D. J. Joswiak, D. E. Brownlee, R. O. Pepin, and D. J. Schlutter: Characterization of asteroidal and cometary IDPs obtained from stratospheric collectors: Summary of measured He release temperature, velocities, and descriptive mineralogy, *Lunar Planet. Sci. XXXI* Abstract #1500 [CD-ROM] (2001).

Publication list related SM/MPAC&SEED

Y. Kitazawa, T. Noguchi, M.J. Neish, I. Yamagata, Y. Kimoto, J. Ishizawa, A. Fujiwara, M. Suzuki, Y. Yamaura, S. Yamane; Passive Measurement of Dust Particles on the ISS (MPAC): Status report of the post flight analysis european Geosciences Union, General Assembly 2007 Vienna, Austria, 15-20 April 2007, CD-ROM (EGU2007-A-01406) (Abstract), (2007).

Y. Kitazawa, M. J. Neish, T. Noguchi, I. Yamagata, Y. Kimoto, J. Ishizawa, A. Fujiwara , M. Suzuki, Y. Yamaura, Y. Watanabe, S. Yamane; Passive measurement of dust particles on the ISS (MPAC): Third report on aerogel dust collectors, 57th Meeting of the Aeroballistic Range Association, Venice, Italy, 18-22 Sept. 2006 CD-ROM , (2007)

T. Noguchi, Y. Kitazawa, M. J. Neish, I. Yamagata, Y. Kimoto, J. Ishizawa, M. Suzuki, A. Fujiwara, Y. Yamaura, S. Yamane; Passive Measurement of Dust Particles on the ISS (MPAC):Fourth report on aerogel dust collectors, Committee on Space Research, 36th COSPAR Scientific Assembly, Beijing, China, 16 -23 July 2006, CD-ROM (PEDAS1-0008-06), (Abstract), (2006)

Y. Kitazawa, M. J. Neish, T. Noguchi, T. Inoue, J. Ishizawa, A. Fujiwara, K. Imagawa, Y. Yamaura, S. Yamane, S. Nakazato; Passive measurement of dust particles on the ISS (MPAC): Second report on aerogel dust collectors, Preprints of The 25th International Symposium on Space Technology and Science, (CD-ROM), Kanazawa, Japan, 30 May - 6 June 2006, (2006)

T. Noguchi, Y. Kitazawa, M. J. Neish, I. Yamagata, Y. Kimoto, J. Ishizawa, M. Suzuki, A. Fujiwara, Y. Yamaura, S. Yamane ; Passive measurement of dust particles on the ISS (MPAC): Third report on aerogel dust collectors, European Geosciences Union General Assembly 2006 Vienna, Austria, 02 - 07 April 2006, CD-ROM (Abstract),(2006)

M. J. Neish, Y. Kitazawa, T. Noguchi, T. Inoue, K. Imagawa, T. Goka, Y. Ochi; Passive measurement of dust particles on the ISS Using MPAC: experiment summary, particle fluxes and chemical analysis, ESA Proceedings of the 4th European Conference on Space Debris, p 221-226, Darmstadt, Germany, 18-20 April 2005 (SP-587, August, 2005), (2005)

Y. Kitazawa, T. Noguchi, M. J. Neish, T. Inoue, J. Ishizawa, A. Fujiwara, K. Imagawa, Y. Yamaura, Y. Watanabe, A. Murakami; First year mission results of passive measurement experiment of dust particles on ISS (MPAC), Preprints of 24th International Symposium on Space Technology and Science, Miyazaki, Japan, 30 May - 6 June 2004 (CD-ROM), (2004)